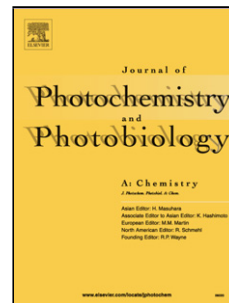


Accepted Manuscript

Title: Synthesis of new triazole based imidazo[1,2-*a*]pyrazine-benzimidazole conjugates: H-bonding assisted FRET efficient ratiometric detection of pyrophosphate

Authors: Richa Goel, Vijay Luxami, Kamaldeep Paul



PII: S1010-6030(17)30666-4
DOI: <http://dx.doi.org/doi:10.1016/j.jphotochem.2017.08.009>
Reference: JPC 10784

To appear in: *Journal of Photochemistry and Photobiology A: Chemistry*

Received date: 16-5-2017
Revised date: 4-8-2017
Accepted date: 6-8-2017

Please cite this article as: Richa Goel, Vijay Luxami, Kamaldeep Paul, Synthesis of new triazole based imidazo[1,2-*a*]pyrazine-benzimidazole conjugates: H-bonding assisted FRET efficient ratiometric detection of pyrophosphate, *Journal of Photochemistry and Photobiology A: Chemistry* <http://dx.doi.org/10.1016/j.jphotochem.2017.08.009>

This is a PDF file of an unedited manuscript that has been accepted for publication. As a service to our customers we are providing this early version of the manuscript. The manuscript will undergo copyediting, typesetting, and review of the resulting proof before it is published in its final form. Please note that during the production process errors may be discovered which could affect the content, and all legal disclaimers that apply to the journal pertain.

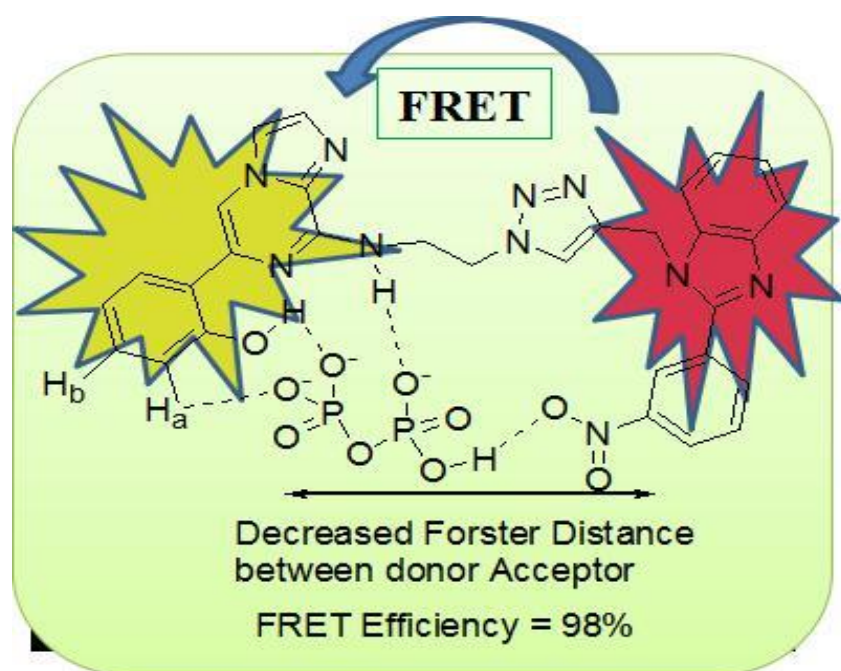
Synthesis of new triazole based imidazo[1,2-*a*]pyrazine-benzimidazole conjugates: H-bonding assisted FRET efficient ratiometric detection of pyrophosphate

Richa Goel, Vijay Luxami* and Kamaldeep Paul*

School of Chemistry and Biochemistry, Thapar University, Patiala-147004, INDIA

*Corresponding Authors. Email Address: vluxami@thapar.edu (V. Luxami);
kpaul@thapar.edu (K. Paul)

Graphical abstract



Highlights

- A series of triazole based imidazo[1,2-*a*]pyrazine-benzimidazole analogs has been synthesized.
- Compounds were synthesized through click and Suzuki reactions.
- Quantum yields of the synthesized compounds were determined.
- FRET efficiency of the molecule has been used for the ratiometric detection of pyrophosphate.

Abstract

Triazole tethered imidazo[1,2-*a*]pyrazine-benzimidazole conjugates **13-38** has been synthesized by click and Suzuki-Miyaura cross coupling reactions at C-8 and C-6 positions, respectively. The research findings clearly predicted that by modification of electronic structure of the receptor, the sensitivity of the recognition process could be modified. Compound **24** with hydroxyphenyl substituent, showed stronger binding to the pyrophosphate than other compounds. Compound **24** has been used as selective probe for ratiometric detection of pyrophosphate amongst the other anions. The binding event of compound **24** toward PPI has been successfully evaluated by absorption and emission spectroscopy as well as NMR titration method. The compound **24** showed H-bonding assisted facilitation of FRET phenomenon in the presence of PPI.

Keywords: Imidazo[1,2-*a*]pyrazine, benzimidazole, click reaction, Suzuki reaction, FRET, pyrophosphate.

1. Introduction

Phosphate-containing anionic species [1] are ubiquitous in biological systems and play important mediatory roles in signal transduction pathways, and carrying genetic informations [2]. For example, pyrophosphate ions (PPI) are involved in energy transduction in organisms, and controlling metabolic processes via participation in enzymatic reactions [3]. Various important biochemical reactions like DNA polymerization, synthesis of cyclic AMP and formation of activated intermediates in protein synthesis, are catalyzed by DNA polymerase, adenylate

cyclase and aminoacyl-tRNA synthetase, respectively. While the hydrolysis of ATP with concomitant release of PPI is an important factor in biochemical pathways [4-6]. Therefore, several research groups have focused on the detection of this biological anion. The design of fluorescent chemosensor for detection of pyrophosphate ion remains a challenge [7-9]. Most of the developed phosphate anion sensors are based on transition metal complexes where the cavity formed by the metal ion with the receptor provides a cooperative binding site for phosphate derivative [10]. In this context, Zn(II) complex has been frequently used for detection of PPI [11-16]. But complexes with other metal ions like Tb(III) [17], Cd(II) [10], Mn(II) [18], Cu(II) [19-25] and Eu(III) [26] have also been employed. Some of these sensors displayed remarkable selectivity and sensitivity. However, considerable synthetic efforts are required for their preparation. Moreover, sensing molecules for detection of PPI are limited in literature and the potential for the development of these PPI sensors are at the primitive stage for bioanalytical applications. Until now, few chemosensors are reported for detection of PPI in the absence of metal ions [27-30].

Amongst different approaches proposed for ratiometric ion sensing, Förster resonance energy transfer (FRET) is a non-radiative energy transfer process in which the excitation energy of the donor is transferred to nearby acceptor via long-range dipole–dipole interaction and/or short-range multipolar interaction. FRET is generally designed as fluorescence sensor to adopt the photophysical changes produced on complexation [31-33]. Recently, FRET based probes [34-35] have been used in cell physiology, optical therapy and selective as well as specific sensing toward target analytes [36-38]. However, despite many advantages, ratiometric sensing of PPI using FRET phenomenon is not known. Imidazo[1,2-*a*]pyrazine is known to exhibit fluorescence properties such as chemiluminescence [39] and bioluminescence [40], found in the scaffold of the Coelenterazine and a bioluminescent compound isolated from the Jellyfish *Aequorea Victoria*. Benzimidazole moiety has been commonly utilized as the molecular recognition site for cation, anion and neutral molecules due to its unique spectral properties. Besides their medicinal uses, imidazopyrazine and benzimidazole derivatives have found technical applications as dyes, electroluminescent materials, organic semiconductors and as suitable ligand in coordination chemistry [41-42]. Keeping above points in consideration, in the present manuscript the two fluorescent moieties have been combined through a spacer as imidazo[1,2-*a*]pyrazine-benzimidazole conjugates for FRET based ratiometric determination of pyrophosphate (PPI).

Moreover, conjugates based on imidazo[1,2-*a*]pyrazine and benzimidazole moieties as sensors have not been reported so far. Herein, we have synthesized these conjugates by implementing click reaction and Suzuki-Miyaura cross coupling reaction at respective C-8 and C-6 positions of imidazo[1,2-*a*]pyrazine and studied their photophysical properties to determine the FRET based ratiometric detection of pyrophosphate. The motivation behind the synthesis of these compounds was to synthesize sensor for biologically important anions. Thus, criterion for choosing the organic moiety was fluorescent electron deficient moiety having nitro group so that it can interact with electron rich anions. In continuation to search for an efficient compound, a series of organic compounds were synthesized to fine tune the FRET efficiency. The compound **24** showed the best quantum yield and FRET efficiency and was chosen for the further study.

2. Experimental

2.1 General Experimental Conditions

All commercially available compounds (Avra, Spectrochem, Aldrich, Merck etc.) were used without further purification. Final reactions were carried out in an oil bath using Microwave Vials (10-15 ml). Melting points were determined in open capillaries and were uncorrected. ^1H and ^{13}C NMR spectra were performed on Jeol ECS 400 NMR spectrometer, which was operated at 400 MHz for ^1H nuclei and 100 MHz for ^{13}C nuclei, using CDCl_3 , $\text{DMSO-}d_6$ and trifluoroacetic acid (TFA) as solvents. Chemical shifts are reported in parts per million (ppm) with TMS as internal reference and J values are given in hertz. 2D NOE studies were performed on same instrument. Mass Spectra of the synthesized compounds were recorded at Water Micromass-Q-T of Micro. Reactions were monitored by thin layer chromatography (TLC) with silica plate coated with silica gel HF-254 and column chromatography was performed with silica gel 60-120/100-200 mesh. Ethylacetate and methanol were adopted solvent systems.

2.1.1 General procedure for synthesis of compounds **4** and **5**:

2-Bromoethylamine hydrobromide / 3-bromopropylamine hydrobromide (4.90 mmol) was dissolved in distilled water with stirring. Sodium azide was added (13.84 mmol) carefully to this solution in succession with continuous stirring. The reaction mixture was refluxed for 12 h. After completion of reaction, reaction mixture was cooled to room temperature and was quenched by

addition of sodium hydroxide (17.5 mmol) and further stirred for 30 min at room temperature. Thereafter, mixture was extracted with diethyl ether and dried over sodium sulphate to obtain ether extract and stored at low temperature. The ether extract being volatile in nature, was used as such for next reaction.

2.1.2 General procedure for synthesis of compounds **6** and **7**:

To the ether extract containing **4** or **5** was added to the solution of 6,8-dibromoimidazo[1,2-*a*]pyrazine **1** (1.80 mmol) in acetonitrile in the presence of diisopropylethylamine (DIPEA). The reaction mixture was refluxed for 24 h. After completion of reaction, the mixture was extracted with chloroform and water. Organic layer was separated, dried over sodium sulphate, filtered and concentrated under vacuum. The crude mixture was then purified by silica gel chromatography 60-120 mesh using hexane: ethyl acetate (8:2) as eluents.

2.1.3 Synthesis of 2-(3-nitrophenyl)-1-(prop-2-ynyl)-1H-benzo[*d*]imidazole (**9**):

To 2-(3-nitrophenyl)-1H-benzo[*d*]imidazole **8** (4.08 mmol) was added 80% solution of propargyl bromide in toluene (8.40 mmol) in the presence of potassium carbonate (4.08 mmol) and DMF. The mixture was stirred at room temperature for 12 h. Completion of reaction was monitored by TLC. Reaction was quenched by addition of ice cold water. The solid product was filtered to obtain pure off white solid **9**.

2.1.4 General procedure for synthesis of compounds **10** and **11**:

To a stirred solution of 2-(3-nitrophenyl)-1-(prop-2-ynyl)-1H-benzo[*d*]imidazole **9** (3.6 mmol) and **6** or **7** (3.6 mmol) in 50 ml ethanol:water (8:2), copper sulphate pentahydrate (5 mol%) and sodium ascorbate (10 mol%) were added and stirred at room temperature for 2 h. After completion of reaction, water was added and extracted with chloroform. Chloroform layer was dried over anhydrous sodium sulphate, filtered and concentrated in vacuum to obtain pure solid **10** or **11**.

2.1.5 General procedure for synthesis of compounds **13-38**:

To a solution of **10** or **11** (0.178 mmol) in mixture of 1,4-dioxane : water (9:1) in a sealed tube, boronic acid (0.178 mmol) and K₂CO₃ (0.178 mmol) were added under inert atmosphere. Then,

[Pd(PPh₃)₄] (5mol%) was added with continued nitrogen purging. Sealed the tube and refluxed the reaction mixture for 6-8 h. Completion of reaction was determined by TLC. The mixture was extracted with chloroform and water. Organic layer was dried over sodium sulphate to obtain crude product which was further purified by column chromatography to get pure products **13-38**.

2.2 Photophysical measurements

All photophysical measurements were performed in acetonitrile. Absorption spectra were measured with a UV-2500, Shimadzu spectrophotometer. Fluorescent measurements were performed with a Carry Eclipse spectrophotometer. The quantum yields of the imidazo[1,2-*a*]pyrazine analogues were determined relative to anthracene.

2.3 Fluorescence quantum yield

The fluorescence quantum yield Φ_{fs} for all compounds was determined at room temperature in analytical grade CH₃CN using anthracene ($\Phi_{fr} = 0.22$) in acetonitrile as the standard. The quantum yield was calculated by using eqn--1, in which Φ_{fs} is the radiative quantum yield of the sample, Φ_{fr} is the radiative quantum yield of reference, A_s and A_r are the absorbance of the sample and the reference, respectively, D_s and D_r are the areas of emission for the sample and reference respectively, L_s and L_r are the lengths of the absorption cells, and N_s and N_r are the refractive indices of the respective sample and reference solutions (pure solvents were assumed).

$$\phi_{fs} = \phi_{fr} \times \frac{1 - 10^{-A_r L_r}}{1 - 10^{-A_s L_r}} \times \frac{N_s^2}{N_r^2} \times \frac{D_s}{D_r} \quad \text{-----1}$$

3. Results and discussion

3.1 Chemistry

Imidazo[1,2-*a*]pyrazine-benzimidazole conjugates have been synthesized by the reaction of 2-aminopyrazine and *N*-bromosuccinimide at room temperature followed by cyclization with chloroacetaldehyde at 110 °C for 72 h to obtain 6,8-dibromoimidazo[1,2-*a*]pyrazine **1** in 80% yield. Compound **1** was then reacted with 2-azidoethanamine **4** and 3-azidopropanamine **5** [43-44] (obtained from reaction of 2-bromoethylamine hydrobromide **2** and 3-bromopropylamine hydrobromide **3** with sodium azide for 12 h at reflux temperature followed by stirring with

sodium hydroxide), to afford respective *N*-(2-azidoethyl)-6-bromoimidazo[1,2-*a*]pyrazin-8-amine **6** in 72% yield and *N*-(3-azidopropyl)-6-bromoimidazo[1,2-*a*]pyrazin-8-amine **7** in 65% yield (Scheme 1). These azides have low thermal stability, so, these were stored in ether or hexane at low temperature.

On the other hand, reaction of 2-(3-nitrophenyl)-1*H*-benzo[*d*]imidazole **8** with propargyl bromide, in the presence of potassium carbonate and DMF at room temperature for 12 h obtained 2-(3-nitrophenyl)-1-(prop-2-ynyl)-1*H*-benzo[*d*]imidazole **9** in 95% yield (Scheme 2).

Keeping both the precursors, copper catalyzed azide-alkyne cycloaddition (CuAAC) reaction was performed by reacting azides **6** and **7** with alkyne **9** in the presence of copper sulphate and sodium ascorbate at room temperature for 2 h to afford imidazo[1,2-*a*]pyrazine-benzimidazole conjugates **10** and **11** in 81% and 85% yields, respectively (Scheme 3).

However, a mixture of 1,4-disubstituted triazole **10** and 1,5-disubstituted triazole **12** in 2:1 ratio was obtained with reaction of azide **6** and alkyne **9** on heating without using any catalyst. It has been observed that thermal [2+3] dipolar cycloaddition of alkyne to azide is not a regiospecific reaction [45]. NOESY experiment was carried out to confirm the formation of 1,4 and 1,5-disubstituted products. Positive NOE was observed between the protons of triazole at C-5' and alkyl groups at N-1' and C-4' positions in compound **10**, suggesting that the triazole proton and both alkyl groups are in close proximity. On the other hand, No NOE signal was observed between the C-4' proton of triazole and alkyl group at N-1' position in 1,5-disubstituted triazole **12**. However, positive NOE signal was observed between triazole proton at C-4' and C-5' substituted alkyl group (Figure 1).

Conjugate **10** was further reacted with various of aryl boronic acids through Suzuki-Miyaura cross coupling at C-6 position of imidazo[1,2-*a*]pyrazine using Pd(PPh₃)₄ and K₂CO₃, providing library of arylated compounds **13-28** (Scheme 4, Table 1). Several electron donating and electron withdrawing groups were introduced on aryl group of imidazo[1,2-*a*]pyrazine. The reactions were well tolerated with five member rings viz., thiophen-2-yl (**13**), thiophene-3-yl (**14**) and furan-2-yl (**15**). Substitution with electron withdrawing groups on phenyl ring such as 4-fluorophenyl (**17**), 4-chlorophenyl (**18**), 4-bromophenyl (**19**), 3-trifluoromethylphenyl (**20**), 4-formylphenyl (**27**) and 4-acetylphenyl (**28**) gave good yields of products while electron donating groups, 3-methylphenyl (**21**) and 2-methoxy phenyl (**26**) were obtained in moderate yields. Increase in yield was also observed with methoxy substitution from ortho (**26**) to para position

(25) of phenyl ring. Similarly, compounds **29-38** were obtained by the reaction of compound **11** with different aryl boronic acids (Scheme 4, Table 1). The chemical structures were fully characterized by ^1H and ^{13}C NMR as well as mass spectrometry (Figures S1-S64, Supporting Information, File 1).

In case of halogen containing compounds, the electron withdrawing group such as 3-(trifluoromethyl)phenyl moiety in **20** and **33** gave good quantum yields (0.53 and 0.62, respectively) in comparison to other halogenated compounds **17** (0.14), **18** (0.38) and **19** (0.38). On increasing linker length from ethyl to propyl as exemplified by compounds **20** and **27** with **33** and **38**, increase in quantum yields were observed. FRET efficiency based upon the fluorescence quantum yield has also been determined. The FRET efficiency (η) was evaluated using the equation $\eta = 1 - \Phi_{F(\text{donor in dyad})} / \Phi_{F(\text{free donor})}$. Here, $\Phi_{F(\text{donor in dyad})}$ is the fluorescence quantum yield of donor part in dyad and $\Phi_{F(\text{free donor})}$ is the fluorescence quantum yield of donor when not connected to acceptor. It has been observed that presence of some electron donating substituents showed lower FRET efficiencies in comparison to electron withdrawing substituents. However, the maximum FRET efficiency (92%) from donor part of dyad to acceptor part was displayed by compound **24** with 2-hydroxyphenyl substituent attached at the acceptor part.

Imidazo[1,2-*a*]pyrazine behaved as an acceptor and showed absorption band at 360 nm. There was a significant spectral overlap between absorption spectra of the imidazo[1,2-*a*]pyrazine (acceptor) and emission spectra of the benzimidazole (donor) (Figures 2, S65 and S66). Dyad **24** showed the emission band at 365 nm with $\Phi_f = 0.95$ and $\eta = 92\%$. Keeping in view, due to maximum quantum yield and FRET efficiency of compound **24** amongst other series of compounds, the effect of various anions like F^- , Cl^- , Br^- , I^- , AcO^- , H_2PO_4^- , NO_3^- , CN^- , SCN^- , HSO_4^- , S^{2-} , CO_3^{2-} , SO_3^{2-} and PPI was studied on compound **24**.

The addition of various anions (100 μM) *viz.*, F^- , Cl^- , Br^- , I^- , CN^- , H_2PO_4^- , NO_3^- , AcO^- , HSO_4^- , SCN^- , S^{2-} , CO_3^{2-} , SO_3^{2-} , etc. and metal ions such as Cu^{2+} , Zn^{2+} , Co^{2+} , Ni^{2+} , Al^{3+} , Fe^{3+} , Cr^{3+} etc. caused insignificant change in absorption spectrum of dyad **24** (Figures S67, S68). However, the presence of PPI ions induced the formation of new absorption band. The titration of solution of dyad **24** (20 μM , CH_3CN) with PPI showed a gradual decrease in absorbance at 286 nm associated with an increase in absorbance at 370 nm with an isobestic point at 340 nm. Appearance of absorption band at 370 nm in the presence of PPI could be attributed due to intramolecular charge transfer (ICT).

A plot of log [PPi] concentration Vs A_o/A showed a linear increase in absorbance between 10^{-6} - 10^{-5} M PPi. The “*On-Off-On*” behavior at 286 nm and 370 nm has been used for the ratiometric estimation of PPi (Figure 3, S69) [46]. The time dependence response of the sensor was checked over the varied time. The absorption changes attained by the sensor were intact over the period of 24 hrs (Figure S70).

The solution of dyad **24** (CH_3CN , 20 μM) upon excitation at λ_{ex} 280 nm exhibited emission maxima at 365 nm. Upon addition of aliquot of PPi, the fluorescence intensity at 365 nm was gradually quenched and associated with red shift of emission maxima to 430 nm (Figure 4). The dyad **24** initially showed the emission at 365 nm typically due to benzimidazole moiety. In the presence of PPi, new emission band appeared at 430 nm typically due to imidazopyrazine which clearly showed that in the presence of PPi excited benzimidazole moiety transfers its energy to imidazopyrazine through FRET and started giving imidazopyrazine emission at 430 nm. The addition of all other anions (100 μM) viz., F^- , Cl^- , Br^- , I^- , CN^- , H_2PO_4^- , NO_3^- , AcO^- , HSO_4^- , SCN^- etc. caused insignificant change in the emission of dyad **24** (Figure S71).

The selectivity of dyad **24** towards PPi was further ascertained by the competition experiment where competing anions viz., Cl^- , Br^- , I^- , CN^- , H_2PO_4^- , NO_3^- , AcO^- , HSO_4^- , SCN^- etc. were added to the solution of dyad **24** before addition of PPi. As predicted from the results, the FRET efficiency in the presence of PPi remained by and large unaffected in the presence of several interfering anions. This indicates that dyad **24** is selective for recognition of PPi even in the presence of other anions (Figure S72) The lowest detection limit for PPi estimation was found to be 0.2 μM .

Further insight and quantitative evaluation of the sensing capability of compounds **10**, **11** and **13-38** (20 μM , CH_3CN) with pyrophosphate was obtained from UV-vis and fluorescence experiments (Figures S73 and S74, Supporting information). It was surprising that only compound **24** with 2-hydroxyphenyl ring at C6 position of imidazo[1,2-*a*]pyrazine, showed significant change with pyrophosphate indicating that 2-hydroxyphenyl moiety is responsible for binding with PPi. The formation of new emission band could be attributed to intramolecular interaction in the excited state of the hydroxyphenyl and benzimidazole moieties facilitated in the presence of coordinated PPi. The distance between the hydroxyphenyl and benzimidazole moieties in absence of PPi was closer to Förster distance and thus showed 92% FRET efficiency, whereas presence of PPi, decrease the Förster distance and hence FRET efficiency is increased to 98%.

In an effort to gain more detailed information of the interaction between compound **24** and PPI, ^1H NMR titration study was carried out in CD_3CN (Figure 5). The assignments of protons of compound **24** have been confirmed by 2D NOESY and COSY NMR experiments (Figures S35-S36). The proton signal at δ 8.1 was attributed to the 2-hydroxyphenyl proton H_a . Signal at δ 7.2 was due to overlapping triplets from the characteristic protons H_b and H_c , and signal at δ 7.5 was due to proton H_d of hydroxyphenyl moiety. Protons of OH at δ 12.8 and NH_c at δ 6.8 disappeared on the addition of 0.5 equivalent of PPI. Proton H_a adjacent to the hydroxyl group broadened and shifted downfield by 1.2 ppm (8.1-9.3 ppm) until the end of the titration experiment (over two equivalents of PPI added). The large shifting as well as broadening of signal might be due to hydrogen bonding of compound **24** with pyrophosphate (Figure 5). The signal of the other proton H_d is separated out and shifted downfield by 0.4 ppm (7.5-7.9 ppm) upon addition of pyrophosphate ion. Moreover, two double doublets at δ 8.2 and 8.3 of nitrobenzene in benzimidazole are also approaching towards each other. This interesting behavior of compound **24** could be explained by considering the important contribution given by the benzimidazole and 2-hydroxyphenyl in assisting the interaction of the receptor and pyrophosphate anion. On the basis of ^1H NMR studies of compound **24** with pyrophosphate, the proposed binding modes for compound **24** with PPI is shown in Figure 6.

4. Conclusions

We have synthesized a series of imidazo[1,2-*a*]pyrazine-benzimidazole conjugates, based upon “click” and “Suzuki-Miyaura cross coupling” reactions. It has been observed that by simply changing the substituents in the acceptor part of conjugate, FRET efficiency of the compound can be tuned. In particular, the substitution with 2-hydroxy phenyl group at C-6 position of imidazo[1,2-*a*]pyrazine (**24**), showed the best FRET efficiency and used for ratiometric detection of pyrophosphate. The fluorescent electron deficient moiety on the benzimidazole ring due to nitro group was also interacted with electron rich anions. Thus, the compound **24** showed the best quantum yield as well as FRET efficiency. Only few organic compounds in the absence of metal complexes have been reported in literature for the detection of PPI. The present manuscript described the first organic compound for the PPI sensing with FRET phenomenon and having good detection limit (Table S1).

Supporting Information

Additional information, characterization methods, experimental, analytical data, and copies of NMR spectra.

Acknowledgements

KP thanks DST, New Delhi (EMR/2014/000669) and UGC, New Delhi (41-322/2012, SR) for providing funds. RG is indebted to CSIR for SRF (09/677(0020)/2013.EMR-I). SAI labs, Thapar University is also acknowledged for recording NMR spectra.

Notes and References

1. J.K. Heinonen, Biological role of inorganic pyrophosphate, Kluwer Academic Publishers, Boston, 2001.
2. J.A. Drewry, S. Fletcher, H. Hassan, P.T. Gunning, Novel asymmetrically functionalized bis-dipicolylamine metal complexes: peripheral decoration of a potent anion recognition scaffold, *Org. Biomol. Chem.* 7 (2009) 5074-5077.
3. C.P. Mathews, K.E. van Hold, Biochemistry, The Benjamin/Cummings Publishing Company, Inc., Redwood City, CA, 1990.
4. W.N. Limpcombe, N. Sträter, Recent advances in zinc enzymology, *Chem. Rev.* 96 (1996) 2375-2434.
5. P. Nyrén, Enzymatic method for continuous monitoring of DNA polymerase activity, *Anal. Biochem.* 167 (1987) 235-238.
6. T. Tabary, L.Y. Ju, J.H. Cohen, Homogeneous phase pyrophosphate (PPi) measurement (H3PIM). A non-radioactive, quantitative detection system for nucleic acid specific hybridization methodologies including gene amplification, *J. Immunol. Methods*, 156 (1992) 55-60.
7. E.J. O'Neil, B.D. Smith, Anion recognition using dimetallic coordination complexes, *Coord. Chem. Rev.* 250 (2006) 3068-3080.
8. R. Martínez-Manez, F. Sancenón, Fluorogenic and chromogenic chemosensors and reagents for anions, *Chem. Rev.* 103 (2003) 4419-4476.
9. P.D. Beer, P.A. Gale, Anion recognition and sensing: The state of the art and future perspectives, *Angew. Chem. Int. Ed.* 40 (2001) 486-516.
10. S. Mizukami, T. Nagano, Y. Urano, A. Odani, K. Kikuchi, A fluorescent anion sensor that works in neutral aqueous solution for bioanalytical application, *J. Am. Chem. Soc.* 124 (2002) 3920-3925.
11. C. Park, J.-I. Hong, A new fluorescent sensor for the detection of pyrophosphate based on a tetraphenylethylene moiety, *Tetrahedron Lett.* 51 (2010) 1960-1962.

12. X.-h. Huang, Y. Lu, Y.-b. He, Z.-h. Chen, A metal–macrocycle complex as a fluorescent sensor for biological phosphate ions in aqueous solution, *Eur. J. Org. Chem.* (2010) 1921–1927.
13. J.H. Lee, J. Park, M.S. Lah, J. Chin, J.-I. Hong, High-affinity pyrophosphate receptor by a synergistic effect between metal coordination and hydrogen bonding in water, *Org. Lett.* 9 (2007) 3729–3731.
14. H.N. Lee, Z. Xu, S.K. Kim, K.M.K. Swamy, Y. Kim, S.-J. Kim, J. Yoon, Pyrophosphate-selective fluorescent chemosensor at physiological pH: Formation of a unique excimer upon addition of pyrophosphate, *J. Am. Chem. Soc.* 129 (2007) 3828–3829.
15. H.N. Lee, K.M.K. Swamy, S.K. Kim, J.-Y. Kwon, Y. Kim, S.-J. Kim, Y.J. Yoon, J. Yoon, Simple but effective way to sense pyrophosphate and inorganic phosphate by fluorescence changes, *Org. Lett.* 9 (2007) 243–246.
16. A. Ojida, H. Nonaka, Y. Miyahara, S. Tamaru, K. Sada, I. Hamachi, Bis(Dpa-Zn^{II}) appended xanthone: Excitation ratiometric chemosensor for phosphate anions, *Angew. Chem. Int. Ed.* 45 (2006) 5518–5521.
17. C.M.G. dos Santos, T. Gunnlaugsson, The recognition of anions using delayed lanthanide luminescence: The use of Tb(III) based urea functionalised cyclen complexes, *Dalton Trans.* (2009) 4712–4721.
18. K.M.K. Swamy, S.K. Kwon, H.N. Lee, S.M.S. Kumar, J.S. Kim, J. Yoon, Fluorescent sensing of pyrophosphate and ATP in 100% aqueous solution using a fluorescein derivative and Mn²⁺, *Tetrahedron Lett.* 48 (2007) 8683–8686.
19. S. Watchasit, A. Kaowliw, C. Suksai, T. Tuntulani, W. Ngeontae, C. Pakawatchai, Selective detection of pyrophosphate by new tripodal amine calix[4]arene-based Cu(II) complexes using indicator displacement strategy, *Tetrahedron Lett.* 51 (2010) 3398–3402.
20. Z. Guo, W. Zhu, H. Tian, Hydrophilic copolymer bearing dicyanomethylene-4*h*-pyran moiety as fluorescent film sensor for Cu²⁺ and pyrophosphate anion, *Macromolecules*, 43 (2010) 739–744.
21. M.J. Kim, K.M.K. Swamy, K.M. Lee, A.R. Jagdale, Y. Kim, S.-J. Kim, K.H. Yoo, J. Yoon, Pyrophosphate selective fluorescent chemosensors based on coumarin–DPA–Cu(II) complexes, *Chem. Commun.* (2009) 7215–7217.

22. S.Y. Kim, J.-I. Hong, Dual signal (color change and fluorescence ON–OFF) ensemble system based on bis(Dpa-Cu^{II}) complex for detection of PPI in water, *Tetrahedron Lett.* 50 (2009) 1951–1953.
23. X. Huang, Z. Guo, W. Zhu, Y. Xie, H. Tian, A colorimetric and fluorescent turn-on sensor for pyrophosphate anion based on a dicyanomethylene-4*H*-chromene framework, *Chem. Commun.* (2008) 5143–5145.
24. Y.J. Jang, E.J. Jun, Y.J. Lee, Y.S. Kim, J.S. Kim, J. Yoon, Highly effective fluorescent and colorimetric sensors for pyrophosphate over H₂PO₄⁻ in 100% aqueous solution, *J. Org. Chem.* 70 (2005) 9603–9606.
25. L. Fabbrizzi, N. Marcotte, F. Stomeo, A. Taglietti, Pyrophosphate detection in water by fluorescence competition assays: Inducing selectivity through the choice of the indicator, *Angew. Chem. Int. Ed.* 41 (2002) 3811–3814.
26. N. Shao, J. Jin, G. Wang, Y. Zhang, R. Yang, J. Yuan, Europium(III) complex-based luminescent sensing probes for multi-phosphate anions: modulating selectivity by ligand choice, *Chem. Commun.* (2008) 1127–1129.
27. T.-M. Fu, C.-Y. Wu, C.-C. Cheng, C.-R. Yang, Y.-P. Yen, A novel highly selectively colorimetric and fluorescent chemosensor for pyrophosphate ion, *Sens. Actuators B*, 146 (2010) 171–176.
28. Z. Xu, J.-Y. Choi, J. Yoon, Fluorescence sensing of dihydrogen phosphate and pyrophosphate using imidazolium anthracene derivatives, *Bull. Korean Chem. Soc.* 32 (2011) 1371-1374.
29. C. Caltagirone, C. Bazzicalupi, F. Isaia, M.E. Light, V. Lippolis, R. Montis, S. Murgia, M. Olivari, G. Picci, A new family of bis-ureidic receptors for pyrophosphate optical sensing, *Org. Biomol. Chem.* 11 (2013) 2445-2451.
30. P. Sokkalingam, D. S. Kim, H. Hwang, J.L. Sessler, C.-H. Lee, A dicationic calix[4]pyrrole derivative and its use for the selective recognition and displacement-based sensing of pyrophosphate, *Chem. Sci.* 3 (2012) 1819-1824.
31. T. Förster, Zwischenmolekulare energiewanderung und fluoreszenz, *Ann. Phys.* 2 (1948) 55-75.
32. B. W. vander Meer, G. Coker III, S.-Y. Simon Chen, VCH, Weinheim, Germany, 1994

33. P. Mahato, S. Saha, E. Suresh, R. DiLiddo, P.P. Parnigotto, M.T. M.K. Conconi, Kesharwani, B. Ganguly, A. Das, Ratiometric detection of Cr^{3+} and Hg^{2+} by a naphthalimide-rhodamine based fluorescent probe, *Inorg. Chem.* 51 (2012) 1769-1777.
34. J. Wu, W. Liu, J. Ge, H. Zhang, P. Wang, New sensing mechanisms for design of fluorescent chemosensors emerging in recent years, *Chem. Soc. Rev.* 40 (2011) 3483-3495.
35. X. Chen, T. Pradhan, F. Wang, J.S. Kim, J. Yoon, Fluorescent chemosensors based on spiroring-opening of xanthenes and related derivatives, *Chem. Rev.* 112 (2012) 1910-1956.
36. C. Ma, F. Zeng, L. Huang, S. Wu, FRET-based ratiometric detection system for mercury ions in water with polymeric particles as scaffolds, *J. Phys. Chem. B*, 115 (2011) 874-882.
37. B.R. White, H.M. Liljestrand, J.A. Holcombe, A 'turn-on' FRET peptide sensor based on the mercury binding protein MerP, *Analyst*, 133 (2008) 65-70.
38. G. Fang, M. Xu, F. Zeng, S. Wu, β -cyclodextrin as the vehicle for forming ratiometric mercury ion sensor usable in aqueous media, biological fluids, and live cells, *Langmuir*, 26 (2010) 17764-17771.
39. K. Teranishi, T. Nishiguchi, H. Ueda, Enhanced chemiluminescence of 6-(4-methoxyphenyl)imidazo[1,2-*a*]pyrazin-3(7*H*)-one by attachment of a cyclomaltooligosaccharide (cyclodextrin). Attachment of cyclomaltononose (δ -cyclodextrin), *Carbohydr. Res.*, 338 (2003) 987-993.
40. K. Teranishi, Luminescence of imidazo[1,2-*a*]pyrazin-3(7*H*)-one compounds, *Bioorg. Chem.*, 35 (2007) 82-111.
41. P. Molina, A. Tarraga, F. Oton, Imidazole derivatives: A comprehensive survey of their recognition properties, *Org. Biomol. Chem.* 10 (2012) 1711-1724.
42. Z. Xu, S.K. Kim, J. Yoon, Revisit to imidazolium receptors for the recognition of anions: highlighted research during 2006–2009, *Chem. Soc. Rev.* 39 (2010) 1457-1466.
43. N. Song, M. Ding, Z. Pan, J. Li, L. Zhou, H. Tan, Q. Fu, construction of targeting-clickable and tumor-cleavable polyurethane nanomicelles for multifunctional intracellular drug delivery, *Biomacromolecules*, 14 (2013) 4407–4419.
44. S. Angelos, Y.-W. Yang, K. Patel, J.F. Stoddart, J.I. Zink, pH-Responsive supramolecular nanovalves based on cucurbit[6]uril pseudorotaxanes, *Angew. Chem. Int. Ed.* 47 (2008) 2222–2226.

45. C.W. Tornøe, C. Christensen, M. Meldal, Peptidotriazoles on solid phase: [1,2,3]-Triazoles by regiospecific copper(i)-catalyzed 1,3-dipolar cycloadditions of terminal alkynes to azides, *J. Org. Chem.* 67 (2002) 3057-3064.
46. H.A. Benesi, J.H. Hildebrand, A spectrophotometric investigation of the interaction of iodine with aromatic hydrocarbons, *J. Am. Chem. Soc.* 71 (1949) 2703-2707.

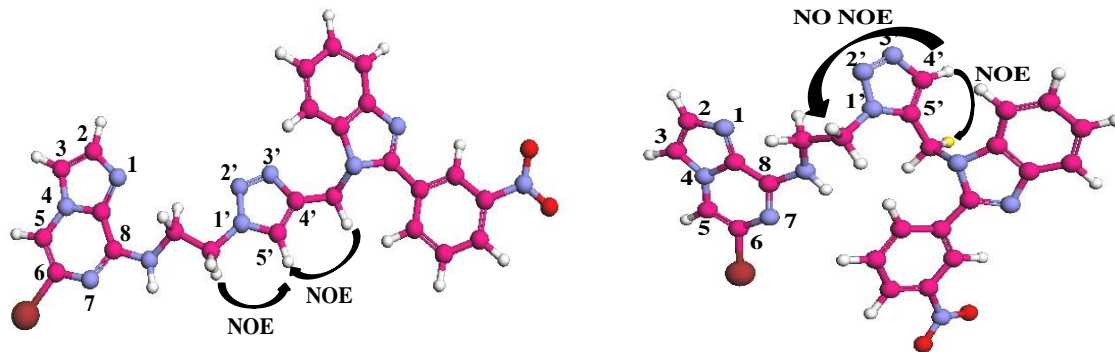


Figure 1 NOE correlation experiments of 1,4-(**10**) and 1,5-(**12**) disubstituted triazoles

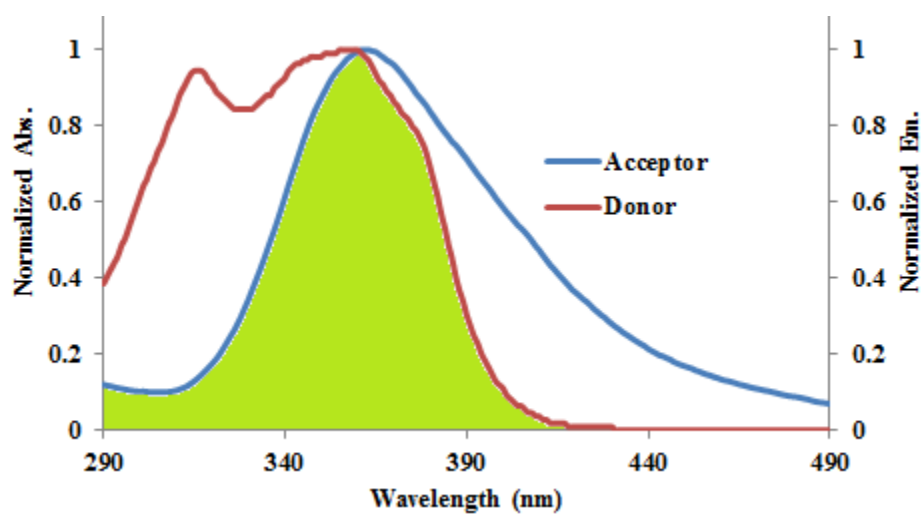


Figure 2: Spectral overlap between absorption spectrum of imidazopyrazine (acceptor, compound **6** ($\Phi_f = 0.08$)) and emission spectrum of benzimidazole (donor, compound **9** ($\Phi_f = 0.1$)).

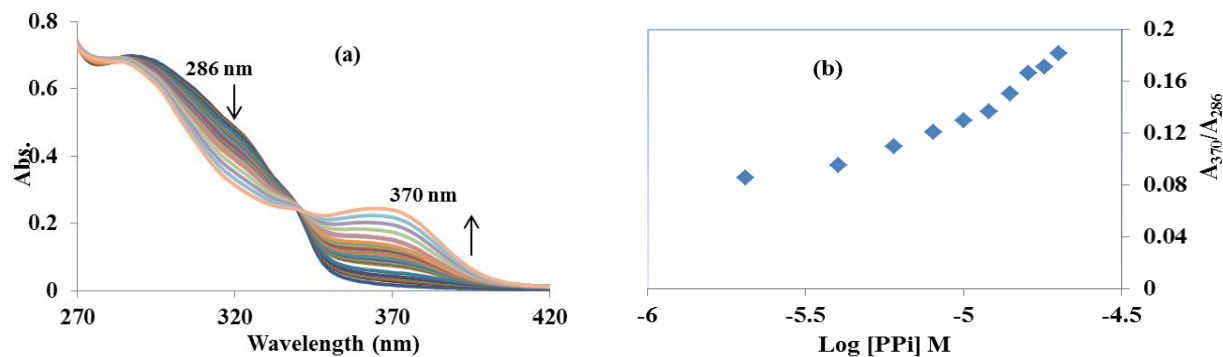


Figure 3: (a) Changes in absorption spectrum of compound **24** (20 μM in CH_3CN) upon addition of tris(tetrabutylammonium) hydrogen pyrophosphate (PPI); (b) Plot of A_{370}/A_{286} vs $\log [\text{PPI}]$ for the ratiometric response of compound **24** towards PPI.

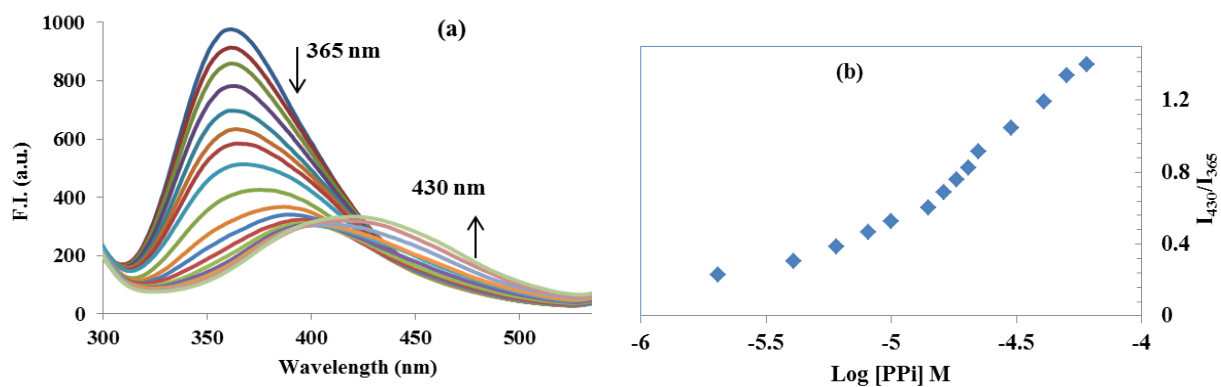


Figure 4: (a) Changes in emission spectrum of compound **24** (20 μM in CH_3CN) upon addition of PPI (0.2 μM to 1000 μM); (b) Plot of I_{430}/I_{365} vs $\log [\text{PPI}]$ for the ratiometric response of compound **24** towards PPI.

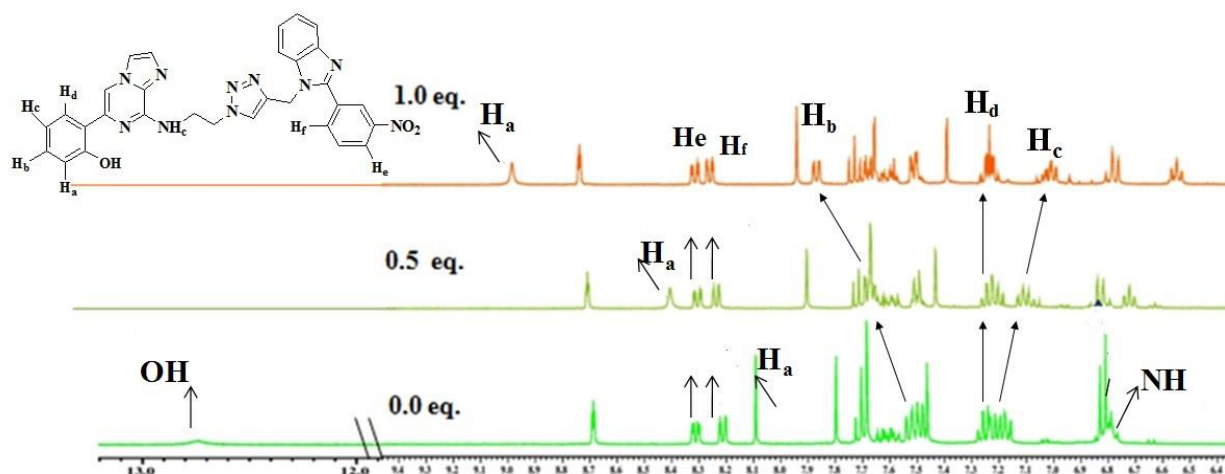


Figure 5: ^1H NMR stack plot of a CD_3CN solution of compound **24** (5 mM) upon addition of tris(tetrabutylammonium)hydrogen pyrophosphate (0.5-1.0 eq.).

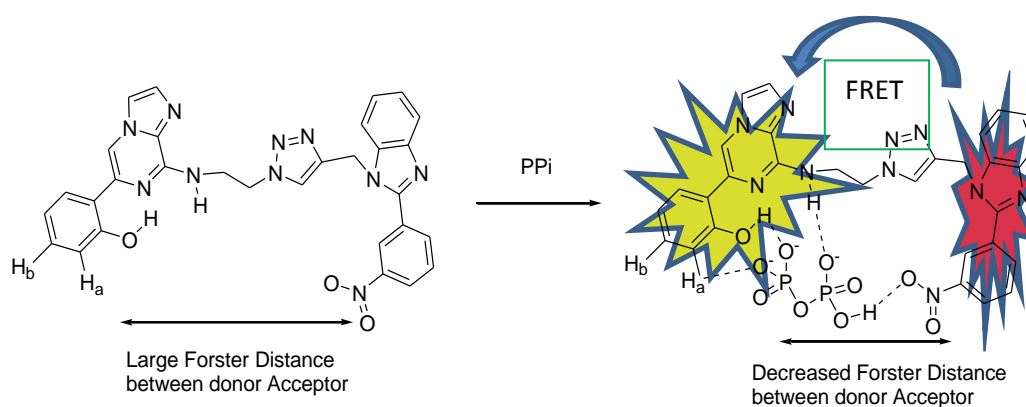
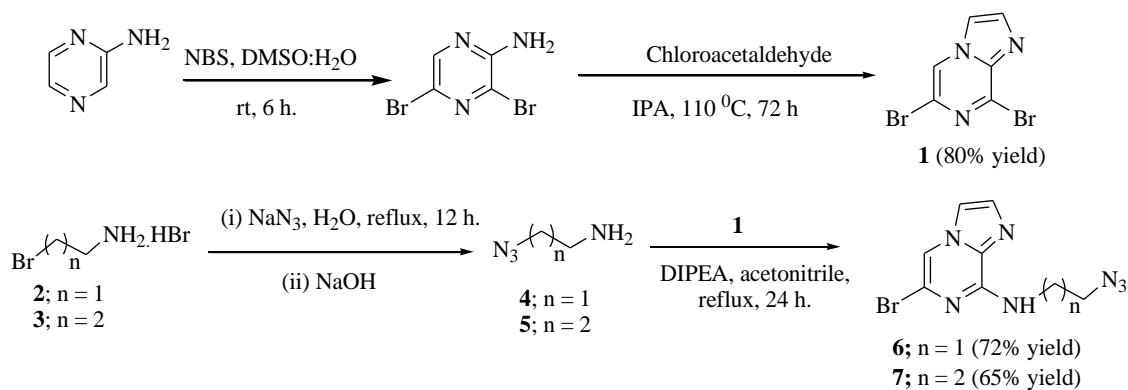
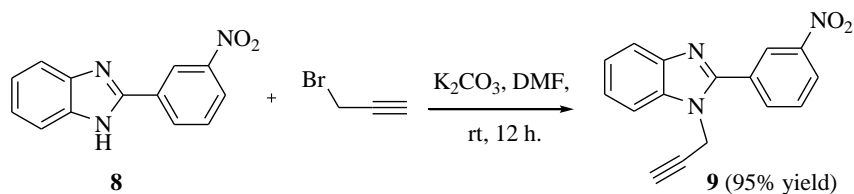


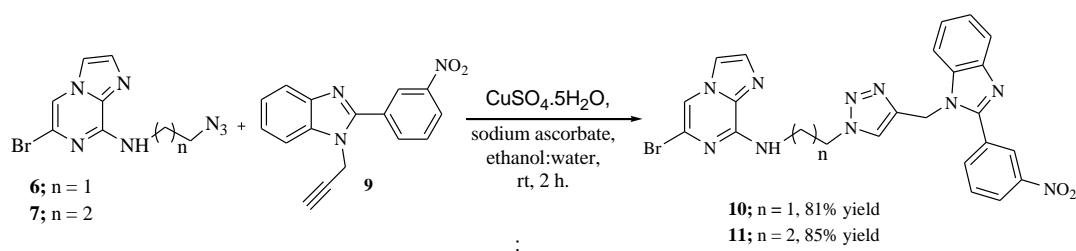
Figure 6: Suggested binding structure for **24** with PPI



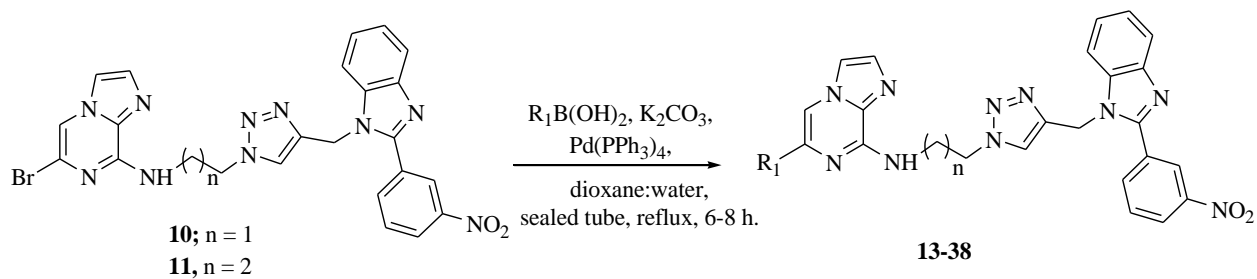
Scheme 1 Synthesis of imidazo[1,2-*a*]pyrazinamine ethyl **6** and propyl **7** azide



Scheme 2 Synthesis of *N*-propargylated benzimidazole **9**



Scheme 3 Synthesis of triazole tethered imidazo[1,2-*a*]pyrazine-benzimidazole conjugates **10** and **11**



Scheme 4 Suzuki-Miyaura coupling of ethyl and propyl triazole tethered imidazo[1,2-*a*]pyrazine-benzimidazole conjugates

Table 1 Suzuki-Miyaura coupling of ethyl **10**, **13-28** and propyl triazole **11**, **29-38** bridged imidazo[1,2-*a*]pyrazine-benzimidazole conjugates and their physiochemical parameters

3.2 Photophysical properties

Compounds **10**, **11** and **13-38** were further studied for their photophysical properties (Table 1). Quantum yields of all compounds were calculated with respect to anthracene in acetonitrile. It has been revealed that presence of electron withdrawing groups viz., 4-formyl phenyl (**27** and **38**) and 4-acetyl phenyl (**28**) gave excellent quantum yields (0.90, 0.92 and 0.85, respectively).

Compound	Time (h)	R ₁	n	Yields (%)	$\lambda_{\max}^{\text{abs}}$ (nm)	$\lambda_{\max}^{\text{emi}}$ (nm)	ϵ	Φ_{r}	FRET efficiency
10	4	bromo	1	81	287	375	36600	0.22	85.3
13	8	thiophen-2-yl	1	73	286	420	42250	0.19	87.3
14	8	thiophen-3-yl	1	81	288	366	46250	0.13	91.3
15	8	furan-2-yl	1	62	288	375	36200	0.26	82.6
16	6	phenyl	1	80	291, 280	408	53800	0.52	65.3
17	7	4-fluorophenyl	1	73	282	365	47250	0.14	90.6
18	7	4-chlorophenyl	1	79	284	380	56050	0.38	72.6
19	7	4-bromophenyl	1	84	283	380	50450	0.38	74.6
20	6	3-(trifluoromethyl)phenyl	1	69	283	395	50400	0.53	64.6
21	6	3-methylphenyl	1	61	285	406	50250	0.32	62.6
22	6	4-ethylphenyl	1	77	283	385	57700	0.28	81.3
23	8	naphthalen-1-yl	1	55	285	420	55050	0.11	25.3
24	8	2-hydroxyphenyl	1	43	286	365	26600	0.95	92.0
25	7	4-methoxyphenyl	1	91	286, 258	373	66950	0.15	90.0
26	6	2-methoxyphenyl	1	58	289	407	37550	0.48	45.3
27	6	4-formylphenyl	1	88	340, 274	496	47300	0.90	ND
28	8	4-acetylphenyl	1	71	340, 272	475	59750	0.85	ND
11	6	bromo	2	85	287	365	28100	0.15	90.3
29	8	thiophen-3-yl	2	68	287	368	30300	0.28	81.3
30	8	phenyl	2	67	288	405	30400	0.70	53.3
31	8	4-fluorophenyl	2	76	282	370	28350	0.14	90.6
32	6	4-chlorophenyl	2	78	284	390	32550	0.41	74.6
33	7	3-(trifluoromethyl)phenyl	2	53	283	392	17800	0.62	18.6
34	7	3-methylphenyl	2	57	284	372	22750	0.56	78.6
35	8	4-ethylphenyl	2	62	283	371	37000	0.36	76.0
36	6	4-methoxyphenyl	2	81	286, 258	372	31800	0.43	71.3
37	6	2-methoxyphenyl	2	83	289	370	34950	0.82	71.0
38	6	4-formylphenyl	2	80	341, 274	505	31250	0.92	ND